Boletín de la Sociedad Geológica Mexicana
Volumen 68, núm. 2, 2016, p. 323-338

Provenance of opaque minerals in coastal sands, western Gulf of Mexico, Mexico

Juan José Kasper-Zubillaga[1,*], Carlos Linares López[2], Carmen Adela Espino de la Fuente Muñoz[3]

[1] Instituto de Ciencias del Mar y Limnología, Universidad Nacional Autónoma de México, Unidad Académica de Procesos Oceánicos y Costeros, Circuito Exterior s/n, CP 04510, Ciudad Universitaria. Ciudad de México, México.
[2] Departamento de Vulcanología, Instituto de Geofísica, Universidad Nacional Autónoma de México, Ciudad Universitaria, 04510, Ciudad de México, México.
[3] Ingeniería en Geología Ambiental, Universidad Autónoma del Estado de Hidalgo, Carretera Pachuca - Actopan Km. 4.5 7o. Piso, Colonia Campo de Tiro, 42039 Pachuca, Hidalgo, México.

[*] kasper@cmarl.unam.mx

Abstract

This paper contributes to the study of the provenance of opaque minerals (OM), *i.e*., ilmenite, titanomagnetite, and magnetite in beach and dune sands from the western coast of the Gulf of Mexico. Grain sizes in the sands are controlled by a wide coastal plain that also influences their distribution. The quartzose nature of the beach and dune sands from the western coast of the Gulf of Mexico is derived from Upper Cretaceous and Tertiary shales and sandstones exposed along the coast from the Miramar to the Tepehuajes beach sites and from denudation cycles from the Sierra de Tamaulipas which is composed of intrusive rocks. This is supported by the presence of sandstones, chert, monocrystalline quartz with straight extinction, K-feldspars, amphiboles, and pyroxenes. The OM subordinate fractions in the beach and dune sands studied show that ilmenite is primarily derived from pre-existing eroded mafic sources, *i.e.*, alkali basalts originating from the Aldama and Sierra de Maratínez volcanic field sites that are exposed close to the Miramar beach. The primary sources of titanomagnetite and magnetite subordinate fractions come from subalkaline basalts from the Aldama rocks low in K-feldspar with an increase in Ca-plagioclase and also from granites from the Sierra de Tamaulipas, respectively. The OM grains like ilmenite, titanomagnetite, and magnetite are subrounded, and from rounded to very rounded, suggesting longshore transport, breaking wave influence, and wind deflation effect from the source rock to the beach site.

Keywords: opaque minerals (OM), ilmenite, titanomagnetite, magnetite, beach, dune sands, roundness, Gulf of Mexico, Mexico.

Resumen

El presente trabajo determina la procedencia de minerales opacos (MO) como la ilmenita, titanomagnetita y magnetita en arena de playa y duna en la costa oeste del Golfo de México. La distribución del tamaño de grano de la arena está influido por una planicie costera ancha. El carácter cuarzoso de la arena de playa y duna de la costa oeste del Golfo de México proviene de lutitas y areniscas del Cretácico Superior y Terciario expuestos a lo largo de la costa desde la playa Miramar hasta la playa Tepehuajes producto de la erosión de la Sierra de Tamaulipas compuesta por rocas intrusivas. Esto se encuentra sustentado por la presencia de fragmentos de areniscas, pedernal, cuarzo microcristalino con extinción recta, feldespato de potasio, anfíboles y piroxeno. Los MO subordinados en la arena de playa y duna muestran que la ilmenita proviene de la erosión de rocas fuente como basaltos alcalinos del campo volcánico de Aldama y de la Sierra de Maratínez cerca de la playa de Miramar. La fuente primaria de cristales subordinados de titanomagnetita y magnetita proviene de basaltos subalcalinos de las rocas basálticas de Aldama con menor contenido de feldespato de potasio y aumento en plagioclasa cálcica y también de los granitos de la Sierra de Tamaulipas, respectivamente. Los MO como la ilmenita,

titanomagnetita y magnetita son subredondeados y redondeados a muy redondeados lo cual implica transporte a lo largo de la costa, influencia de la energía del oleaje y deflación de la arena en la costa desde la roca fuente hasta la playa.

Palabras clave: minerales opacos (MO), ilmenita, titanomagnetita, magnetita, playa, duna, arena, redondez, Golfo de México, México.

1. Introduction

Opaque minerals (OM) such as ilmenite ($FeTiO_3$), titanomagnetite defined as a solid solution between ulvöspinel (Fe_2TiO_4) and magnetite (Fe_3O_4) can be used as provenance tracers in sedimentary terranes due to their relative stability in volcanic and coastal sands (Darby and Tsang, 1987; Grigsby, 1990; Kasper-Zubillaga *et al*., 2013). Additionally, OM are useful in provenance and coastal process studies because of their variable concentrations in major and trace elements, especially in TiO_2, and their relative stability during sand transport, which provides information on source rocks and coastal processes (Grigsby, 1990; Butler, 1992; Fletcher *et al*., 1992; Bradley *et al*., 2002; Kasper-Zubillaga *et al*., 2008a, b; Armstrong-Altrin *et al*., 2012; Nallusamy *et al*., 2013; Makvandi *et al*., 2015).

The purpose of this paper is to determine the provenance of OM in beach and dune sands of the western coast of the Gulf of Mexico surrounded by mafic volcanic, volcanoclastic rocks and subordinate exposures of felsic intrusive bodies. OM in the beach and dune sands from the western coastal area of the Gulf of Mexico were studied due to their similar geomorphological characteristics to coastal areas elsewhere, *i.e*., wide sandy strandplains, some with vegetated dune systems (Komar and Wang, 1984; Bradley *et al*., 2002; Angusamy, 2006; Dill, 2007). In this paper we discuss the extent to which OM in beach and dune sands from the Gulf of Mexico are geochemically controlled by the geology of the surrounding area. In order to prevent bias focusing on one single detrital-mineral population (in our case OM) representing a minimal part of the total sediment input seawards (Garzanti, 2016), our approach considered the bulk composition of the coastal sands, including: a) the grain size characteristics of the coastal sands, b) the petrographic analysis of light minerals (*i.e.*, quartz, feldspars, and rock fragments) (Kasper-Zubillaga *et al.*, 2013), c) the geochemistry of the OM, for provenance purposes, and d) the roundness of the grains, in order to observe the degree to which the subordinate OM are close to the source rocks or have experienced longshore transport away from the source rocks.

2. Study areas

The study area is located in the State of Tamaulipas, on the western coast of the Gulf of Mexico, Mexico (Figure 1). The three beaches sampled, from south to north, were Miramar, Barra del Tordo, and Tepehuajes (Figure 1). Sand dunes are of the vegetated-transverse type (Livingstone *et al*., 1999). The three beach sites are located 74 to 51 km apart with an average width of 130 ± 29.9 m, 50 ± 19.6 m, and 43.3 ± 6.5 m ($\rho = 0.05$; n = 3) for each beach, respectively (INEGI, 2012).

The sedimentary rocks exposed in the area belong to the Gulf of Mexico Coastal Plain between the Sierra Madre Oriental (Tpal (lu)) and the Gulf of Mexico coast, composed of Upper Cretaceous and Tertiary shales and sandstones along the three beach sites studied. The Volcanic rocks, *i.e*., the Aldama and Maratínez extrusive igneous rocks (T (Igeb) and Q (Igeb)) of mid to late Tertiary and/or Quaternary ages, respectively, are exposed near the Barra del Tordo and Tepehuajes beach sites (Treviño-Cázares *et al*., 2005; Aranda-Gómez *et al*., 2007). Their chemical composition ranges from trachytes to alkali basalts, *i.e.*, ~ 47 to 60 % SiO_2; ~ 5 to 15 % $Na_2O + K_2O$ (Le Maitre *et al*., 2002; Aranda-Gómez *et al*., 2007) (Figure 1). The Sierra de Tamaulipas intrusive igneous rocks intruded in Cretaceous limestones west of the Aldama and Maratínez rocks. They are composed of alkaline intrusions, *i.e*., gabbro to granite (T (Igia)) (Ortega-Gutiérrez *et al*., 1992; Aranda-Gómez *et al*., 2007).

Tides in the study area are semidiurnal, averaging 50 and 30 cm in amplitude for the three beach sites (Yáñez-Arancibia and Day, 2005). Longshore currents are 13 cm/s and 7 cm/s during the dry and wet seasons, respectively (Fernández-Eguiarte *et al*., 1992). Waves measure on average 0.6 to 1.2 m in height, with periods of 6 to 8 s, and they move in a northerly direction.

Winds come from the north, east, northeast, and southeast with average velocities of 4, 3, 5, and 4 m/s per year, respectively (Pérez-Villegas, 1990). Average annual precipitation ranges from 300 to 2000 mm (INEGI, 2012). Average temperatures range from 28 to 30 °C in summer and from 14 to 20 °C in the winter (Yáñez-Arancibia and Day, 2005).

3. Equipment and methods

3.1. Field sampling

Beach and dune sands were collected from Miramar (n = 35), Barra del Tordo (n = 55), and Tepehuajes (n = 35)

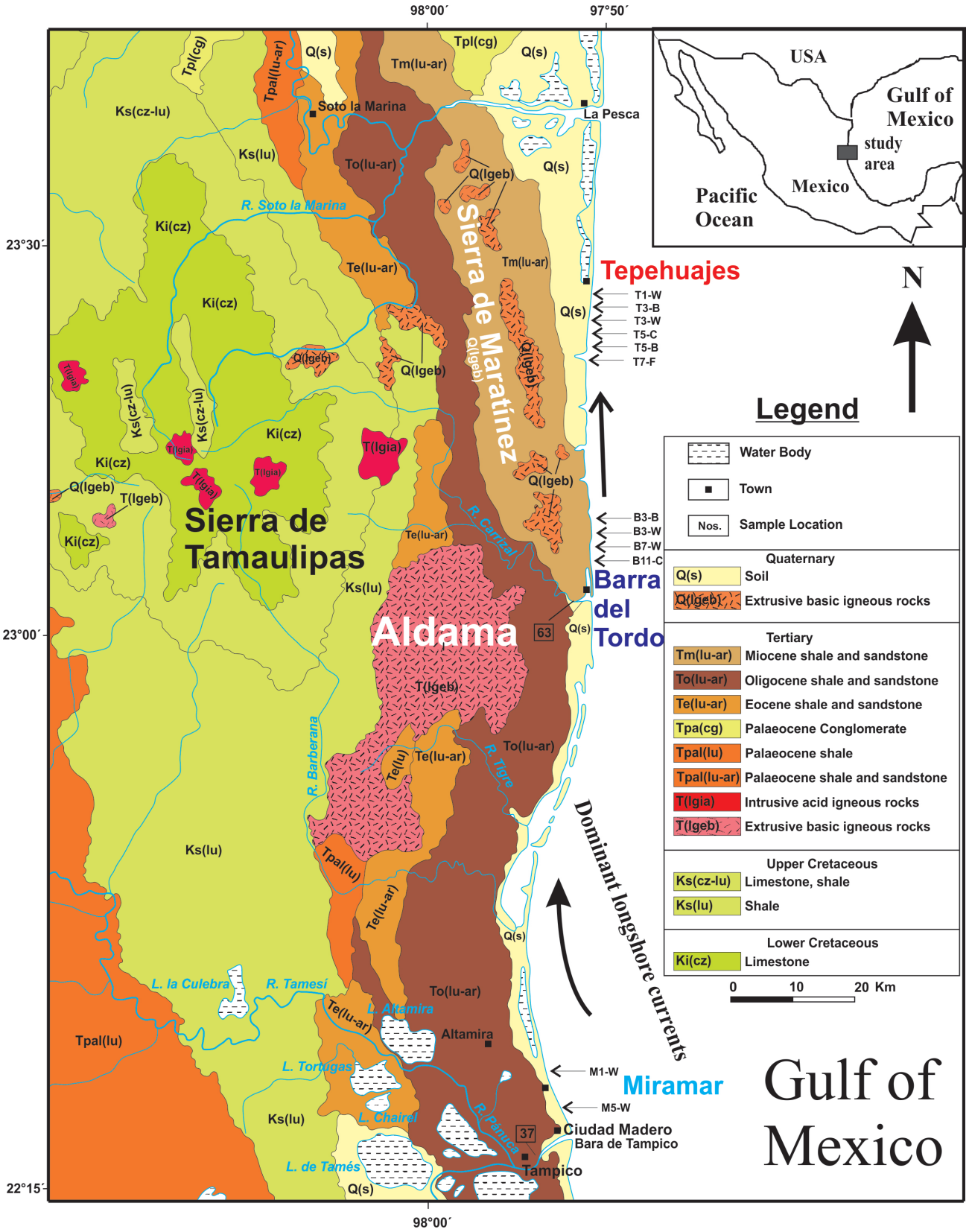

Figure 1. Geological map and sampling sites (map modified and taken from the Mexican Geological Service, 2015).

during the wet season *i.e*., August 2012. Samples were taken from the uppermost centimeter of the inshore, foreshore, and backshore of the beach. Samples were also taken from the windward side and the crest of the dune sands. This was performed in order to prevent bias in grain size and mineral composition of the sands since each beach and dune subenvironment are controlled by a combination of coastal processes, *i.e*., longshore currents, wind deflation, and wave energy (Komar and Inman, 1970; Abuodha, 2003; Kasper-Zubillaga *et al*., 2013, 2015).

3.2. Sand petrography

Compositional modes from the Miramar and Barra del Tordo beach sites were taken from a previous study conducted by Kasper-Zubillaga *et al.* (2013). Sand samples from Tepehuajes beach and dune sands were point-counted in this study following the method described by Franzinelli and Potter (1982). This was done because of a) the size (Mz ϕ) and b) the sorting (σ ϕ) character of the sands. Further results regarding these two parameters are shown in subsection 4.1. Normalized rock fragment point-counting results were plotted in a ternary diagram with Rv and Rs (volcanic and sedimentary lithic fragments plotted separately) were associated with a supracrustal influence, while the Rm + Rp (metamorphic and plutonic lithic fragments grouped together) pole was associated with a deep-seated crust (see Kasper-Zubillaga *et al*., 2013). Modal analysis of the whole bulk sand composition, *i.e*., point counting of 200 to 300 grains per slide, included: total quartz (Qt) = mono and polycrystalline quartz; total feldspar; (Ft) = K-feldspar (Fk) + plagioclase (P); and total rock fragments (Rt) = volcanic + sedimentary + metamorphic + plutonic lithics; heavy minerals (HM), mainly magnetite with few zircon grains; and biogenic components (B) like shells.

3.3. OM separation

OM fractions were subsampled using the sieving sets between 2.00 ϕ to 3.75 ϕ. This was done prior to the grain-size parameter determinations for the whole bulk sand sample due to their usefulness in selecting the sand fractions for heavy mineral separation. Heavy mineral fractions were obtained using 0.2, 0.4, 0.8, and 1.2 amperage at tilting variable 10° to 20° with ~ 40 g of weighted sand sample at the start of the magnetic separation (Bradley *et al*., 2002).

The opaque minerals/non-opaque minerals (OM/NO) ratio was calculated for beach and dune sand samples in order to determine the concentration of ilmenite, titanomagnetite, and magnetite grains for the three beach sites. The OM/NO ratio was produced as the quotient of the fractions expressed in grams obtained with the magnetic separator. Samples displaying the highest values for the OM/NO ratio were selected to be randomly analyzed with a JEOL SuperProbe Microprobe Analyzer (MASP). Details of the analytical results are given in Tables 1 and 2.

OM compositions were plotted in the TiO_2-FeO-Fe_2O_3 ternary diagram (Butler, 1992) (Table 1; Figures 2, 3, 4). Normalization of the data was based on Fe, Ti, and trace element content reported as oxides based on the MASP results (Table 2). Confidence regions of the population mean (CRPM) were drawn at 99 % confidence levels to determine if the means of the three OM groups, *i.e.*, ilmenite, titanomagnetite, and magnetite, were significantly different (Weltje, 2002).

3.4. OM morphology (roundness)

In order to estimate the roundness of the OM, between 50 to 200 OM grains for beach and dune sands were counted.

Table. 1. Simplified data from the MASP analysis of relative abundances of OM in the beach and dune sands, western coast of the Gulf of Mexico.

Sample	ϕ	Ilmenite	Titanomagnetite	Magnetite	Other trace minerals	Remarks
M1-W	2.64	8	4	-----	Chromite, zircon (2)*	*some rare earth elements in zircon *i.e.,* Ce, La, Dy, Tb
M5-W	2.66	3	7	-----	Zircon (5)*	* observed as inclusions in one ilmenite grain
B3-B	2.59	10	5	-----	-----	-----
B3-W	2.53	8	3	1	Chromite, sphene, zircon	-----
B7-W	2.36	8	3	-----	Sphene, zircon	-----
B11-C	2.5	12	2	-----	Sphene	-----
T1-W	2.21	4	8	-----	Rutile	
T3-B	2.53	7	4	2	Zircon*	* zircon in ilmenite
T3-W	1.76	5	6	1	Zircon (2)	-----
T5-C	2.43	3*	2*	3	Zircon (5)	*ilmenite overgrowth in one titanomagnetite grain
T5-B	2.51	2	10*	1	Zircon (2)	*titanomagnetite grain with higher TiO_2 concentration in lamellae
T7-F	2.57	9	3	1*	Sphene, zircon	*magnetite with titanomagnetite lamellae

Average sand sizes in ϕ = phi units used for magnetic separation. M = Miramar, B = Barra del Tordo, T = Tepehuajes. Beach sands F = foreshore, B = backshore. Dune sands W = windward, C = crest. Number of trace minerals > 1 are between brackets.

Table 2. Semiquantitative chemical analysis of the OM grains based on the MASP analysis.

Sample	Na_2O	MgO	Al_2O_3	SiO_2	K_2O	CaO	TiO_2	Cr_2O_3	MnO	FeO	ZrO_2	Total
M1-W												
Ilmenite	0	0.73	0.02	0	0.21	0.13	57.31	0.33	0.68	40.57	0	99.98
Ilmenite	0.44	0	0.11	0.32	0.11	0	51.06	0	1.5	46.43	0	99.97
Ilmenite	0.56	0	0.12	0	0.022	0.13	56.29	0	2.35	39.96	0.54	99.97
Ilmenite	0	0.21	0	0.23	0.12	0.49	51.52	0	2.79	44.6	0	99.96
Ilmenite	0	0.15	0	0	0.009	0.05	57.39	0.08	2.6	39.68	0	99.959
Ilmenite	0	0	0	0	0	0	52.18	0	0.6	47.05	0.15	99.98
Ilmenite	0.46	0.56	0	0.27	0.09	0.12	52.85	0	2.72	42.87	0	99.94
Ilmenite	0.13	1.12	0	0.081	0	0.26	55.58	0	0.8	42.01	0	99.981
Average	0.2	0.35	0.03	0.11	0.07	0.15	54.27	0.05	1.76	42.9	0.09	99.97
Sd	0.24	0.42	0.05	0.14	0.08	0.16	2.65	0.12	0.97	2.87	0.19	0.01
Confidence levels	0.17	0.29	0.04	0.1	0.05	0.11	1.83	0.08	0.67	1.99	0.13	0.01
Titanomagnetite	0.93	2.73	1.68	0	0.054	0	34.89	0	0.45	59.21	0	99.944
Titanomagnetite	0.31	0.41	0.57	0	0	0.05	31.03	0	0.32	66.7	0.58	99.97
Titanomagnetite	0	0.76	0.03	0	0	0	28.46	0.05	0.39	70.26	0.01	99.96
Titanomagnetite	0.27	0.46	0.39	0	0	0.16	15.2	0.27	0.23	82.98	0	99.96
Average	0.38	1.09	0.67	0	0.01	0.05	27.4	0.08	0.35	69.79	0.15	99.96
Sd	0.39	1.1	0.71	0	0.03	0.08	8.55	0.13	0.09	9.93	0.29	0.01
Confidence levels	0.39	1.08	0.7	0	0.03	0.07	8.38	0.13	0.09	9.73	0.28	0.01
M5-W												
Ilmenite	1.4	0	0.06	0.17	0	0.2	51.71	0.36	0.52	45.56	0	99.98
Ilmenite	0.28	0.06	0	0.01	0.04	0.18	51.72	0	1.45	45.39	0	99.13
Ilmenite	0.64	0.26	0.3	0.19	0	0.05	50.8	0	0.78	46.82	0.12	99.96
Average	0.77	0.11	0.12	0.12	0.01	0.14	51.41	0.12	0.92	45.92	0.04	99.69
Sd	0.57	0.14	0.16	0.1	0.02	0.08	0.53	0.21	0.48	0.78	0.07	0.48
Confidence levels	0.65	0.15	0.18	0.11	0.03	0.09	0.6	0.24	0.54	0.88	0.08	0.55
Titanomagnetite	0	0.88	1.05	0.52	0	0	8.17	0.42	0.84	87.5	0.57	99.95
Titanomagnetite	0.17	0.36	1.36	0.16	0.04	0	17.15	0.22	0.57	79.94	0	99.97
Titanomagnetite	0.33	0.67	0	0.17	0.02	0.03	31.24	0	0.07	67.43	0	99.96
Titanomagnetite	0	0	0.09	0	0	0.015	6.34	0	0.18	92.7	0.64	99.965
Titanomagnetite	0.4	0.65	0.48	0.13	0.14	0.07	35.76	0.16	0.67	61.36	0.14	99.96
Titanomagnetite	0.04	0.05	0.11	0.05	0.09	0.24	30.68	0	0	68.7	0	99.96
Titanomagnetite	0.41	0.77	1.09	0	0.05	0.13	10.62	0.15	0.54	85.98	0.21	99.95
Average	0.19	0.48	0.6	0.15	0.05	0.07	19.99	0.14	0.41	77.66	0.22	99.96
Sd	0.19	0.35	0.56	0.18	0.05	0.09	12.32	0.15	0.32	11.89	0.27	0.01
Confidence levels	0.14	0.26	0.42	0.13	0.04	0.07	9.13	0.11	0.24	8.81	0.2	0.01
B3-B												
Ilmenite	0	0.03	0	0.55	0	0	52.19	0.47	3.81	42.93	0	99.98
Ilmenite	0.92	0.07	0.29	0	0.19	0.35	60.24	0.22	0.69	36.99	0	99.96
Ilmenite	0.01	0.57	0.1	0.17	0	0.16	51.2	0	1.01	46.74	0	99.96
Ilmenite	0	0	0.27	0.46	0.1	0.19	48.86	0.25	9.36	40.48	0	99.97
Ilmenite	0.56	1.41	0.29	0	0	0	53.9	0.57	2.42	40.81	0	99.96
Ilmenite	0.24	0	0.85	1.15	0	0.64	89.66	0.19	0.03	7.21	0	99.97
Ilmenite	0.23	1.11	0.29	0	0.08	0	51.98	0.12	0	46.16	0	99.97
Ilmenite	0	0.86	0	0	0.1	0.47	48.04	0.49	5.06	44.95	0	99.97
Ilmenite	0	0	0	0	0	0	49.66	0.82	2.37	47.13	0	99.98
Ilmenite	1.05	1.15	0	0.48	0	0.02	54.74	0	1.36	41.17	0	99.97
Average	0.3	0.52	0.21	0.28	0.05	0.18	56.05	0.31	2.61	39.46	0	99.97
Sd	0.4	0.57	0.26	0.38	0.07	0.23	12.32	0.27	2.87	11.79	0	0.01
Confidence levels	0.25	0.35	0.16	0.24	0.04	0.14	7.63	0.17	1.78	7.31	0	0
Titanomagnetite	0	0	0.47	0	0.36	0	31.79	0.7	1.03	65.62	0	99.97
Titanomagnetite	0	2.22	0.53	0	0.1	0	40.89	0	0.33	55.9	0	99.97
Titanomagnetite	0	0.87	0	0	0	0.39	32.94	0.48	0.29	65.01	0	99.98
Titanomagnetite	0.73	0.84	1.53	0	0.2	0	29.62	0	0	67.06	0	99.98
Titanomagnetite	0	2.42	1.57	0.24	0	0	19.93	0.23	1.28	74.3	0	99.97
Average	0.15	1.27	0.82	0.05	0.13	0.08	31.03	0.28	0.59	65.58	0	99.97
Sd	0.33	1.02	0.7	0.11	0.15	0.17	7.53	0.31	0.54	6.56	0	0.01
Confidence levels	0.29	0.9	0.61	0.09	0.13	0.15	6.6	0.27	0.48	5.75	0	0
B3-W												
Ilmenite	0	1.09	0	0	0	0.24	49.86	0.08	0.58	48.12	0	99.97
Ilmenite	0.09	0	0	0.16	0.31	0	52.12	0.07	1.69	45.53	0	99.97
Ilmenite	0.4	3.08	0.03	0.29	0.28	0.44	51.76	0.02	0.83	42.82	0	99.95
Ilmenite	1.23	0.31	0.35	0	0.01	0	56.14	0	0.4	41.53	0	99.97
Ilmenite	0.52	0.61	0	0.89	0.01	0	50.03	0	1.05	46.85	0	99.96
Ilmenite	0	1.66	0	0	0	0.06	53.06	0	1.51	43.7	0	99.99
Ilmenite	0	2.37	0.16	0.05	0.48	0.02	54.08	0.13	0	42.67	0	99.96
Ilmenite	0	0.26	0	0.49	0	0.13	50.89	0.24	0.01	47.95	0	99.97
Average	0.28	1.17	0.07	0.24	0.14	0.11	52.24	0.07	0.76	44.9	0	99.97

Table 2 (continuation). Semiquantitative chemical analysis of the OM grains based on the MASP analysis.

Sample	Na_2O	MgO	Al_2O_3	SiO_2	K_2O	CaO	TiO_2	Cr_2O_3	MnO	FeO	ZrO_2	Total
Sd	0.43	1.11	0.13	0.32	0.19	0.16	2.13	0.08	0.63	2.56	0	0.01
Confidence levels	0.3	0.77	0.09	0.22	0.13	0.11	1.48	0.06	0.44	1.78	0	0.01
Titanomagnetite	0.12	0.79	0.51	0.76	0	0.25	31.67	0	0.22	65.64	0	99.96
Titanomagnetite	1.04	0.74	0	0.27	0.24	0	43.07	0.38	0.25	53.99	0	99.98
Titanomagnetite	0.94	1.3	0.16	1.03	0.05	0.17	15.77	0.02	0.56	79.96	0	99.96
Average	0.7	0.94	0.22	0.69	0.1	0.14	30.17	0.13	0.34	66.53	0	99.97
Sd	0.5	0.31	0.26	0.39	0.13	0.13	13.71	0.21	0.19	13.01	0	0.01
Confidence levels	0.57	0.35	0.3	0.44	0.14	0.14	15.52	0.24	0.21	14.72	0	0.01
Magnetite	0.54	0.06	3.63	5.81	0.04	0.14	3.86	0.58	0.19	85.09	0	99.94
B7-W												
Ilmenite	0	1.26	0.13	0.34	0	0	51.75	0.37	1.03	45.1	0	99.98
Ilmenite	0.02	0.21	0.02	0.35	0	0	52.49	0.08	1.31	45.49	0	99.97
Ilmenite	0.06	1.63	1	0.83	0.17	0.07	50.31	0	0.89	45	0	99.96
Ilmenite	0.15	2.27	0	0	0.01	0.1	52.54	0	0.2	44.7	0	99.97
Ilmenite	0	1.14	0.35	0	0.14	0	52.91	0	0.26	45.18	0	99.98
Ilmenite	0	1.16	0	0.32	0.07	0	50.83	0	0.52	47.07	0	99.97
Ilmenite	0	2.39	0	0.74	0	0.07	51.57	0.24	0.48	44.48	0	99.97
Ilmenite	0	0.83	0	0	0	0.2	31.08	0.14	0.75	66.35	0.62	99.97
Average	0.03	1.36	0.19	0.32	0.05	0.06	49.19	0.1	0.68	47.92	0.08	99.97
Sd	0.05	0.72	0.35	0.33	0.07	0.07	7.37	0.14	0.39	7.49	0.22	0.01
Confidence levels	0.04	0.5	0.24	0.23	0.05	0.05	5.11	0.1	0.27	5.19	0.15	0
Titanomagnetite	1.13	0.64	1.59	0.02	0	0.01	21.86	0.59	0.64	73.47	0	99.95
Titanomagnetite	0	0.32	1.34	0.18	0	0	10.66	0.38	0.52	86.57	0	99.97
Titanomagnetite	0	2.07	2.3	0.14	0	0.02	20.94	0.48	0.43	73.58	0	99.96
Average	0.38	1.01	1.74	0.11	0	0.01	17.82	0.48	0.53	77.87	0	99.96
Sd	0.65	0.93	0.5	0.08	0	0.01	6.22	0.11	0.11	7.53	0	0.01
Confidence levels	0.74	1.05	0.56	0.09	0	0.01	7.04	0.12	0.12	8.52	0	0.01
B11-C												
Ilmenite	0.28	1.2	0	0	0	0.05	52.95	0.39	0.28	44.07	0.72	99.94
Ilmenite	0.41	2.77	0.31	0.07	0	0.24	53.78	0.19	0.38	41.81	0	99.96
Ilmenite	0	1.91	0.09	0.13	0	0	50.89	0.25	0.61	46.03	0.05	99.96
Ilmenite	0	2.84	0	0.44	0	0.34	51.29	0	0.05	44.71	0.24	99.91
Ilmenite	0.3	0.61	0.25	0.44	0	0.05	52.64	0.03	1.11	44.53	0	99.96
Ilmenite	0	0.6	0.04	0	0	0	53.28	0.3	0.78	44.67	0.25	99.92
Ilmenite	0.36	2.76	0.27	0.01	0.086	0.023	50.75	0.17	0.79	44.75	0	99.969
Ilmenite	0	1.83	0.019	0	0	0.1	50.88	0	0.61	45.51	0.85	99.799
Ilmenite	0	2.28	0.01	0	0	0	50.48	0	0.58	45.77	0.86	99.98
Ilmenite	0.68	0.97	0	0	0.17	0	51.43	0	0.93	45.62	0.17	99.97
Ilmenite	0.13	3.17	0.39	0.63	0	0.24	51.56	0.29	0.9	42.65	0	99.96
Ilmenite	0.45	2.15	0.11	0.3	0	0.17	52.97	0	0.52	43	0	99.67
Average	0.22	1.92	0.12	0.17	0.02	0.1	51.91	0.14	0.63	44.43	0.26	99.92
Sd	0.23	0.9	0.14	0.22	0.05	0.12	1.14	0.15	0.3	1.33	0.35	0.09
Confidence levels	0.13	0.51	0.08	0.13	0.03	0.07	0.65	0.08	0.17	0.75	0.2	0.05
Titanomagnetite	0	1.55	0.31	0	0.087	0	31.83	0.2	0.7	65.15	0	99.827
Titanomagnetite	0.03	0.02	0.79	0.52	0.05	0	31.5	0.12	0.41	66.29	0.23	99.96
Average	0.02	0.79	0.55	0.26	0.07	0	31.67	0.16	0.56	65.72	0.12	99.89
Sd	0.02	1.08	0.34	0.37	0.03	0	0.23	0.06	0.21	0.81	0.16	0.09
Confidence levels	0.03	1.5	0.47	0.51	0.04	0	0.32	0.08	0.28	1.12	0.23	0.13
T1-W												
Ilmenite	0.88	0.82	0	0.44	0.1	0	50.38	0.03	0.95	46.35	0	99.95
Ilmenite	0.04	2.47	0	0.09	0.24	0	51.46	0.02	0.73	44.91	0	99.96
Ilmenite	0	0.53	0	0.17	0	0.1	51.8	0.17	1.73	45.48	0	99.98
Ilmenite	0	1.45	0.45	0.37	0.23	0	32.61	0.06	0.65	64.15	0	99.97
Average	0.23	1.32	0.11	0.27	0.14	0.03	46.56	0.07	1.02	50.22	0	99.97
Sd	0.43	0.86	0.23	0.16	0.11	0.05	9.32	0.07	0.49	9.3	0	0.01
Confidence levels	0.43	0.84	0.22	0.16	0.11	0.05	9.13	0.07	0.48	9.12	0	0.01
Titanomagnetite	0	0.62	2.8	0.18	0.11	0.45	8.27	0.28	0.6	86.66	0	99.97
Titanomagnetite	0	0.49	0	0	0	0	11.2	0.02	0.58	87.69	0	99.98
Titanomagnetite	0	0.89	1.21	0.29	0	0	10.56	0.31	0.41	86.31	0	99.98
Titanomagnetite	0.68	7.94	31.02	0.11	0	0	4.3	0.4	0.1	55.33	0	99.88
Titanomagnetite	0	0.24	2.6	0.4	0	0.19	7.94	1.92	0.43	86.26	0	99.98
Titanomagnetite	0	1	0.98	0.26	0	0	7.9	0.04	0.78	88.99	0	99.95
Titanomagnetite	0.29	0	0	0.2	0.01	0	8.71	0.34	0.26	90.16	0	99.97
Titanomagnetite	0.34	0.01	0.47	0.27	0	0	8.4	0.21	0.53	89.74	0	99.97
Average	0.16	1.4	4.89	0.21	0.02	0.08	8.41	0.44	0.46	83.89	0	99.96
Sd	0.25	2.67	10.61	0.12	0.04	0.16	2.07	0.61	0.21	11.64	0	0.03
Confidence levels	0.18	1.85	7.35	0.08	0.03	0.11	1.43	0.43	0.15	8.07	0	0.02
T3-B												

Table 2 (continuation). Semiquantitative chemical analysis of the OM grains based on the MASP analysis.

Sample	Na_2O	MgO	Al_2O_3	SiO_2	K_2O	CaO	TiO_2	Cr_2O_3	MnO	FeO	ZrO_2	Total
Ilmenite	0.99	1.28	0	0.45	0.12	0.12	50.26	0	1.09	45.65	0	99.96
Ilmenite	0	0.4	0.27	0	0.18	0	51.47	0	1.36	46.28	0	99.96
Ilmenite	1.07	0.45	0.37	0.77	0	0	49.6	0.48	2.48	44.74	0	99.96
Ilmenite	0.38	0.8	0.26	0	0	0	49.06	0	0.24	48.6	0.65	99.99
Ilmenite	0.27	2.95	0.19	0.58	0.07	0	53.32	0	1.09	41.51	0	99.98
Ilmenite	0	0.13	0	0.34	0	0	52.13	0.35	0.51	46.53	0	99.99
Ilmenite	0.53	2.8	0.08	0.31	0	0	52.63	0.18	1.22	42.21	0	99.96
Average	0.46	1.26	0.17	0.35	0.05	0.02	51.21	0.14	1.14	45.07	0.09	99.97
Sd	0.43	1.16	0.14	0.28	0.07	0.05	1.61	0.2	0.71	2.5	0.25	0.01
Confidence levels	0.32	0.86	0.11	0.21	0.05	0.03	1.19	0.15	0.53	1.85	0.18	0.01
Titanomagnetite	0	0	0.37	0	0.15	0.03	14.83	0	0	84.56	0	99.94
Titanomagnetite	0	0	0	0.19	0	0.06	25.03	0	1.16	73.54	0	99.98
Titanomagnetite	0.04	0.22	0.23	0.45	0.17	0.1	9.18	0.13	0.59	88.84	0	99.95
Titanomagnetite	0	0.17	0.03	0	0.04	0.08	7.03	0	0	92.28	0.34	99.97
Average	0.01	0.1	0.16	0.16	0.09	0.07	14.02	0.03	0.44	84.81	0.09	99.96
Sd	0.02	0.11	0.17	0.21	0.08	0.03	8.04	0.07	0.56	8.15	0.17	0.02
Confidence levels	0.02	0.11	0.17	0.21	0.08	0.03	7.88	0.06	0.55	7.98	0.17	0.02
Magnetite	0	0	6.8	33.51	0.08	37.79	0	0	0	21.78	0	99.96
Magnetite	0	0.34	0.18	0.38	0	0	1.15	0.19	0.62	97.1	0	99.96
Average	0	0.17	3.49	16.95	0.04	18.9	0.58	0.1	0.31	59.44	0	99.96
Sd	0	0.24	4.68	23.43	0.06	26.72	0.81	0.13	0.44	53.26	0	0
Confidence levels	0	0.33	6.49	32.47	0.08	37.03	1.13	0.19	0.61	73.81	0	0
T3-W												
Ilmenite	0	2.34	0.19	0.52	0.4	0.26	50.39	0	0.7	45.18	0	99.98
Ilmenite	0.52	0.81	0.44	0	0	0.3	52.06	0	0	45.83	0	99.96
Ilmenite	0.07	1.92	0.2	0	0.04	0	51.42	0	0.96	45.35	0	99.96
Ilmenite	1.07	2.93	0.31	0.48	0	0.04	51.87	0	0.9	42.36	0	99.96
Ilmenite	0	0.62	0.33	0.34	0.02	0	53.78	0.08	0.66	44.14	0	99.97
Average	0.33	1.72	0.29	0.27	0.09	0.12	51.9	0.02	0.64	44.57	0	99.97
Sd	0.47	0.99	0.1	0.25	0.17	0.15	1.23	0.04	0.38	1.38	0	0.01
Confidence levels	0	0.87	0.09	0.22	0.15	0.13	1.08	0.03	0.33	1.21	0	0.01
Titanomagnetite	0.55	0	0.41	0	0	0	33.09	0	0.5	65.43	0	99.98
Titanomagnetite	0.16	0	0.65	0	0	0.13	29.45	0	0	68.62	0	99.01
Titanomagnetite	0.62	0	0.9	0	0.53	0	9.46	0.24	1.23	86.98	0	99.96
Titanomagnetite	0	0.81	0.11	0.2	0	0.04	27.63	0	0.37	70.81	0	99.97
Titanomagnetite	1.97	1.69	1.76	0	0.32	0.03	6.49	0	0.64	87.06	0	99.96
Titanomagnetite	1.89	0.26	0	0	0	0.017	0	7.104	0	0.428	90.29	99.99
Average	0.87	0.46	0.64	0.03	0.14	0.04	17.69	1.22	0.46	63.22	15.05	99.81
Sd	0.86	0.68	0.64	0.08	0.23	0.05	14	2.88	0.46	32.15	36.86	0.39
Confidence levels	0.69	0.54	0.51	0.07	0.18	0.04	11.2	2.31	0.37	25.72	29.49	0.31
Magnetite	0.32	0.38	0	0.65	0	0.42	1.3	0.39	0	96.5	0	99.96
T5-C												
Ilmenite	0	0	0.25	0	0	0.07	50.2	0	3.12	43.34	0	96.98
Ilmenite	0	1.29	0.14	0.4	0.21	0	33.57	0.3	0.39	63.66	0	99.96
Ilmenite	0.71	0.15	0	0.1	0.12	0	51.81	0.36	1.74	44.97	0	99.96
Average	0.24	0.48	0.13	0.17	0.11	0.02	45.19	0.22	1.75	50.66	0	98.97
Sd	0.41	0.71	0.13	0.21	0.11	0.04	10.1	0.19	1.37	11.29	0	1.72
Confidence levels	0.46	0.8	0.14	0.24	0.12	0.05	11.43	0.22	1.54	12.78	0	1.95
Titanomagnetite	0	0	0.18	0	0	0.01	9.87	0.04	0	89.89	0	99.99
Titanomagnetite	0	0.32	0.51	0	0	0	16.21	0	1.32	81.62	0	99.98
Average	0	0.16	0.35	0	0	0.01	13.04	0.02	0.66	85.76	0	99.99
Sd	0	0.23	0.23	0	0	0.01	4.48	0.03	0.93	5.85	0	0.01
Confidence levels	0	0.31	0.32	0	0	0.01	6.21	0.04	1.29	8.1	0	0.01
Magnetite	0.43	1.02	0.136	0.21	0	0	3.05	0.07	1.37	93.42	0	99.706
Magnetite	0.03	1.02	2.89	0.23	0.07	0.1	4.53	0	0.45	90.64	0	99.96
Magnetite	0	0.13	0	0.77	0	0	1.42	0.05	0.23	97.38	0	99.98
Average	0.15	0.72	1.01	0.4	0.02	0.03	3	0.04	0.68	93.81	0	99.88
Sd	0.24	0.51	1.63	0.32	0.04	0.06	1.56	0.04	0.6	3.39	0	0.15
Confidence levels	0	0.58	1.85	0.36	0.05	0.07	1.76	0.04	0.68	3.83	0	0.17
T5-B												
Ilmenite	0.72	1.81	0.05	0.37	0	0	51.58	0.3	0.22	44.74	0.15	99.94
Ilmenite	0.25	2.68	0.17	0	0	0	52.67	0.21	0.63	43.21	0	99.82
Average	0	2.25	0.11	0.19	0	0	52.13	0.26	0.43	43.98	0.08	99.88
Sd	0.33	0.62	0.08	0.26	0	0	0.77	0.06	0.29	1.08	0.11	0.08
Confidence levels	0	0.85	0.12	0.36	0	0	1.07	0.09	0.4	1.5	0.15	0.12
Titanomagnetite	0	0	0.42	0.15	0	0	8.76	0.21	0.1	89.88	0.44	99.96
Titanomagnetite	0.78	0.48	0	0.32	0	0	30.18	0	0.33	67.52	0.35	99.96
Titanomagnetite	0.38	1.15	2.18	1	0	0	8.22	0.16	0.85	85.44	0.6	99.98

Table 2 (continuation). Semiquantitative chemical analysis of the OM grains based on the MASP analysis.

Sample	Na_2O	MgO	Al_2O_3	SiO_2	K_2O	CaO	TiO_2	Cr_2O_3	MnO	FeO	ZrO_2	Total
Titanomagnetite	0.26	0.11	0	0	0	0	10.37	0	0.29	88.95	0	99.98
Titanomagnetite	0.37	0.14	0	0.07	0	0.26	51.17	0.02	1.82	46.12	0	99.97
Titanomagnetite	0.19	1.07	0.19	0	0.08	0.03	47.23	0.06	0.9	49.79	0.41	99.95
Titanomagnetite	0	0.49	1.4	0	0.06	0.25	7.2	0.23	0.69	88.95	0.7	99.97
Titanomagnetite	0.54	0.35	0.34	0	0	0	22.23	0	0.72	74.58	0.24	99
Titanomagnetite	0.6	0.11	0	0.01	0	0.17	46.38	0	2.25	50.44	0	99.96
Titanomagnetite	0.25	1.04	0.19	0.12	0	0	29.76	0.07	0	68.56	0	99.99
Average	0.34	0.49	0.47	0.17	0.01	0.07	26.15	0.08	0.8	71.02	0.27	99.87
Sd	0.25	0.66	0.13	0.08	0	0.12	11.75	0.05	1.59	12.81	0	0.02
Confidence levels	0	0.41	0.08	0.05	0	0.07	7.28	0.03	0.99	7.94	0	0.01
Magnetite	1.14	0.23	0	0.34	0.11	0.13	2.55	0	1.21	94.27	0	99.98
T7-F												
Ilmenite	0.5	0	0	0	0.2	0	52.17	0.02	0.49	46.59	0	99.97
Ilmenite	2.32	0.18	0.6	0.14	0	0.01	52.78	0	1.21	42.72	0	99.96
Ilmenite	0	0	0	0.15	0.14	0.1	54.15	0	1.55	43.88	0	99.97
Ilmenite	0.35	0	0.12	0	0	0	51.33	0	0.99	47.15	0	99.94
Ilmenite	0.15	1.03	0.66	1.15	0	0.35	69.38	0.04	3.89	23.3	0	99.95
Ilmenite	0	0.22	0.33	0	0.15	0	57.14	0	6.93	35.13	0	99.9
Ilmenite	0.56	0.08	0	0.5	0.31	0	49.31	0	1.2	47.96	0	99.92
Ilmenite	0.22	0.8	0.13	0.18	0	0.23	49.24	0.44	2.87	45.81	0	99.92
Ilmenite	0	0	0	0.18	0	0	49.51	0.45	2.13	47.7	0	99.97
Average	0.46	0.26	0.2	0.26	0.09	0.08	53.89	0.11	2.36	42.25	0	99.94
Sd	0.73	0.39	0.26	0.37	0.12	0.13	6.36	0.19	2.01	8.14	0	0.03
Confidence levels	0	0.25	0.17	0.24	0.08	0.08	4.15	0.13	1.31	5.32	0	0.02
Titanomagnetite	0	0.67	1.53	0.14	0.43	0	24.5	0.33	0.42	71.96	0	99.98
Titanomagnetite	1.54	1.18	0	0	0.04	0.75	42.24	0	2.62	51.56	0	99.93
Titanomagnetite	0	0.35	0.46	1.46	0.28	0.46	8.51	2.4	0.61	85.43	0	99.96
Average	0.51	0.73	0.66	0.53	0.25	0.4	25.08	0.91	1.22	69.65	0	99.96
Sd	0.89	0.42	0.79	0.81	0.2	0.38	16.87	1.3	1.22	17.05	0	0.03
Confidence levels	1.01	0.47	0.89	0.91	0.22	0.43	19.09	1.47	1.38	19.3	0	0.03
Magnetite	0	13.07	9.6	0.58	0	0.08	1.54	0.93	5.07	69.01	0	99.88

M= Miramar ; B= Barra del Tordo; T= Tepehuajes; F= foreshore, B= backshore, W= dunes windward, C= dunes crest

This was done to a) show the degree of roundness of the OM for beach and dune sands at each site studied, and b) determine the degree to which the OM were under the influence of long and/or short transport since roundness is a good indicator of transport and proximity to possible source rocks (Folk, 1980; Sagga, 1993; Kasper-Zubillaga *et al*., 2005). Fifty-four thin sections were used based on the visual chart presented by Powers (1953). OM were classified and counted as VA = very angular, A = angular, SA = subangular, SR = subrounded, R = rounded and VR = very rounded. The roundness ratios VA/A (very angular/angular), SA/SR (subangular/subrounded), and R/VR (rounded/very rounded) were determined to be used as poles in a ternary diagram (Figures 3a, b) (see Kasper-Zubillaga, 2009). OM were undifferentiated in terms of their geochemical composition, which implies that the OM were considered as one group without isolating ilmenites, titanomagnetites, and magnetites separately during the roundness analysis.

4. Results

4.1. Grain size

The coastal sands were moderately to well-sorted fine sands with Mz = 2.09 ± 0.16, σ = 0.53 ± 0.06; Mz = 2.17 ± 0.08, σ = 0.48 ± 0.08; and Mz = 2.08 ± 2.08, σ = 0.81 ± 0.14 for Miramar, Barra del Tordo, and Tepehuajes, respectively. The beach and dune sands showed relatively similar grain size and sorting values for the three beaches with the exception of the sorting values for Tepehuajes, which were slightly higher compared to the Miramar and the Barra del Tordo sands.

4.2. Modal analysis

Previous petrographic analyses showed that Miramar (Q_{90} F_2 R_8 ; n = 46), Barra del Tordo (Q_{92} F_3 R_5 ; n = 41) (Kasper-Zubillaga *et al*., 2013), and Tepehuajes (Q_{96} F_1 R_3; n = 16) beach and dune sands are quartzose composed of quartz, then rock fragments and feldspar. The sedimentary rock fragments were composed of sandstones, shales, and chert. Chert was dominated by a fine cryptocrystalline texture and showed no rhythmic banding resulting from hydrothermal volcanic activity (He and Zhou, 2014). The sedimentary fragments dominate the samples collected at the Miramar, Barra del Tordo, and Tepehuajes beaches with average ranges of 53 – 60 %, 52 – 65 %, 57 – 64 %, respectively (Kasper-Zubillaga *et al*., 2013). Basaltic lithic fragments are characterized by the absence of conspicuous phenocrystals. The presence of phaneritic textures, polycrystalline, quartzo-feldspathic grains are

observed in intrusive fragments, which are subordinate in all analyzed samples, displaying abundances of medium-sized polycrystalline grains with little recrystallization, an absence of sutured and/or crenulated boundaries and straight crystal-to-crystal boundaries as intrusive derived fractions (Voll, 1960; Blatt, 1967). Quartz-rich river loads are close to the Miramar and Barra del Tordo beach sites, *i.e.*, Q_{94} F_2 R_4 and Q_{96} F_1 R_3, respectively, partially controlling the high quartz content in the coastal sands (Kasper-Zubillaga *et al*., 2013). The Tepehuajes beach site is influenced by the Soto La Marina river input but influenced by longshore currents with a northwesterly component (Fernández-Eguiarte *et al*., 1992; Kasper-Zubillaga *et al*., 2013).

4.3. OM at the Miramar beach site

The OM/NO ratios for beach and dune sands are 0.03 ± 0.00, 0.03 ± 0.00; 0.03 ± 0.00, 0.06 ± 0.02; 0.11 ± 0.05, 0.19 ± 0.06 at Miramar, Barra del Tordo, and Tepehuajes, respectively. The TiO_2-FeO-Fe_2O_3 ternary diagram shows the ilmenite fraction slightly above the 50 % ilmenite mark, *i.e.*, ½ $FeTiO_3$. Comparisons of the ilmenite fraction were made between the gabbros from east Greenland, and ilmenite included as subordinate minerals in basalts from eastern India (Vincent and Phillips, 1954; Nageswara-Rao *et al*., 2012). Additionally, the ilmenite CRPM plots slightly above the 50 % ilmenite mark. Titanomagnetite single grain data and their CRPM overlap the ulvöspinel-titanomagnetite mark, but also overlap the titanomagnetite values for basalts formed at high and low temperatures from east India (Nageswara-Rao *et al*., 2012), and extend towards the wüstite-FeO pole (Grigsby, 1990). Depletion of magnetite grains is observed at the Miramar beach site. No overlapping of the CRPM areas for the ilmenite and titanomagnetite data was observed (Figure 2).

4.4. OM at the Barra del Tordo beach site

The TiO_2-FeO-Fe_2O_3 ternary plot shows that the ilmenite data set plot slightly above the 50 % ilmenite mark, as observed for the ilmenite fraction at the Miramar beach site. Similar to the Miramar beach site trends, titanomagnetite single grain data and their CRPM overlap the ulvöspinel-titanomagnetite mark. The titanomagnetite data set tend towards the wüstite-FeO pole (Grigsby, 1990) and overlap with the reported values for basalts formed at high and low

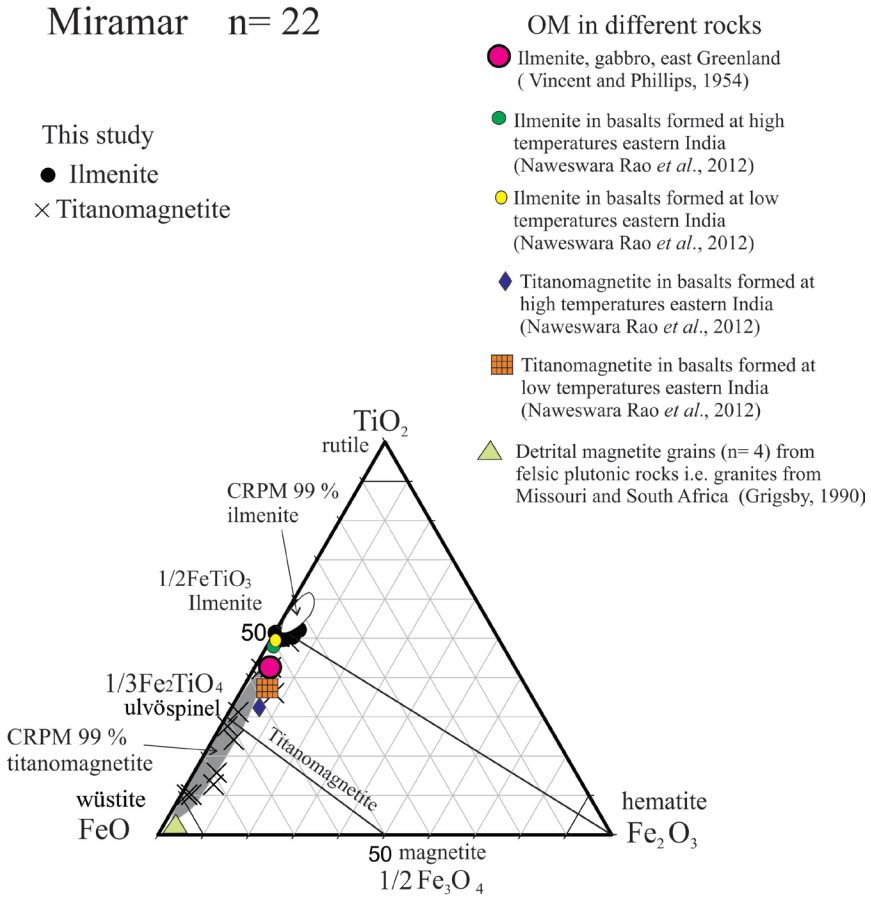

Figure 2. TiO_2-FeO-Fe_2O_3 ternary diagram for Miramar beach and dune sands with ilmenite and titanomagnetite (taken from Butler, 1992). Counted-grains n = 22. Ellipses are CRPM at 99 % confidence levels (Weltje, 2002). See text for explanation.

temperatures in east India (Nageswara-Rao *et al*., 2012) The magnetite samples plot close to the wüstite pole and detrital magnetite grains from intrusive acidic igneous rocks (Grigsby, 1990). The CRPM areas for the ilmenite and titanomagnetite data do not overlap (Figure 3).

4.5. OM at the Tepehuajes beach site

The highest concentration of OM is observed in samples from the Tepehuajes site. The TiO_2-FeO-Fe_2O_3 ternary diagram shows that some ilmenite samples tend towards the rutile pole with high titanium content and slightly above the 50 % ilmenite mark. Some ilmenite samples overlap with the ilmenite in basalts formed at high and low temperatures in eastern India, and slightly above the ilmenite-gabbro association from east Greenland (Vincent and Phillips, 1954; Nageswara-Rao *et al*., 2012). The titanomagnetite minerals plot closer to the wüstite pole while four magnetite grains overlap the detrital magnetite samples comprising granites from the USA (Grigsby, 1990). The rest of the magnetite is spread out towards the magnetite mark and the hematite pole. The CRPM areas for the ilmenite, titanomagnetite, and magnetite grains do not overlap (Figure 4).

4.6. Roundness in OM

The VA/A-SA/SR-R/VR triangular diagram showed that beach sand samples from Miramar and Barra del Tordo tend towards the right-hand side of the triangle, *i.e*., average values > 60 % and 49 %, respectively, near the R/VR pole. The Tepehuajes beach sand samples plot in the middle of the ternary diagram, *i.e.*, average value > 45 % towards the R/VR pole (Figure 5a). The dune sand samples showed more grouping towards the R/VR pole for Miramar and Barra del Tordo than beach sand samples from the same locations, but the Tepehuajes dune sands showed undefined tendencies towards a specific pole with the exception of two dune sand samples that tended towards the SA/SR pole, *i.e.*, average value ~ 40 % towards the SA/SR pole (Figure 5b).

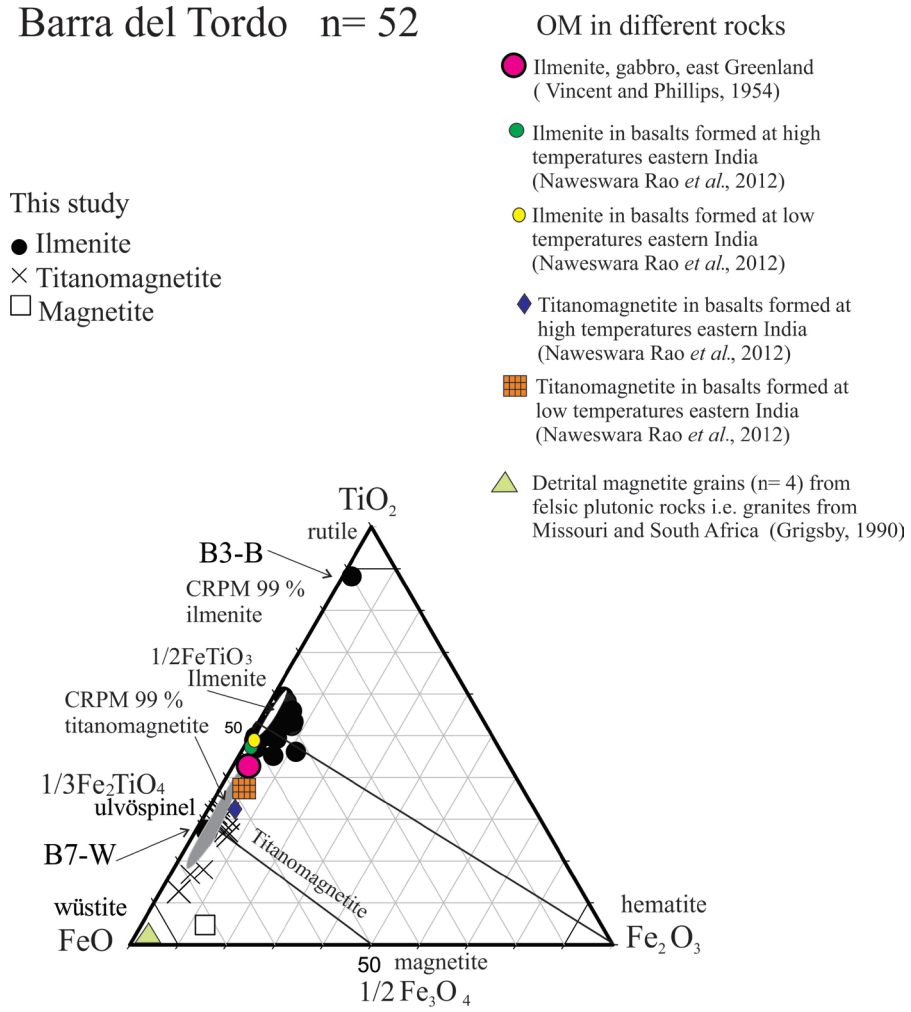

Figure 3. TiO_2-FeO-Fe_2O_3 ternary diagram for Barra del Tordo beach and dune sands with ilmenite and titanomagnetite. Counted-grains n = 52. Ellipses are CRPM at 99 % confidence levels (Weltje, 2002). See Figure 2a and text for explanation.

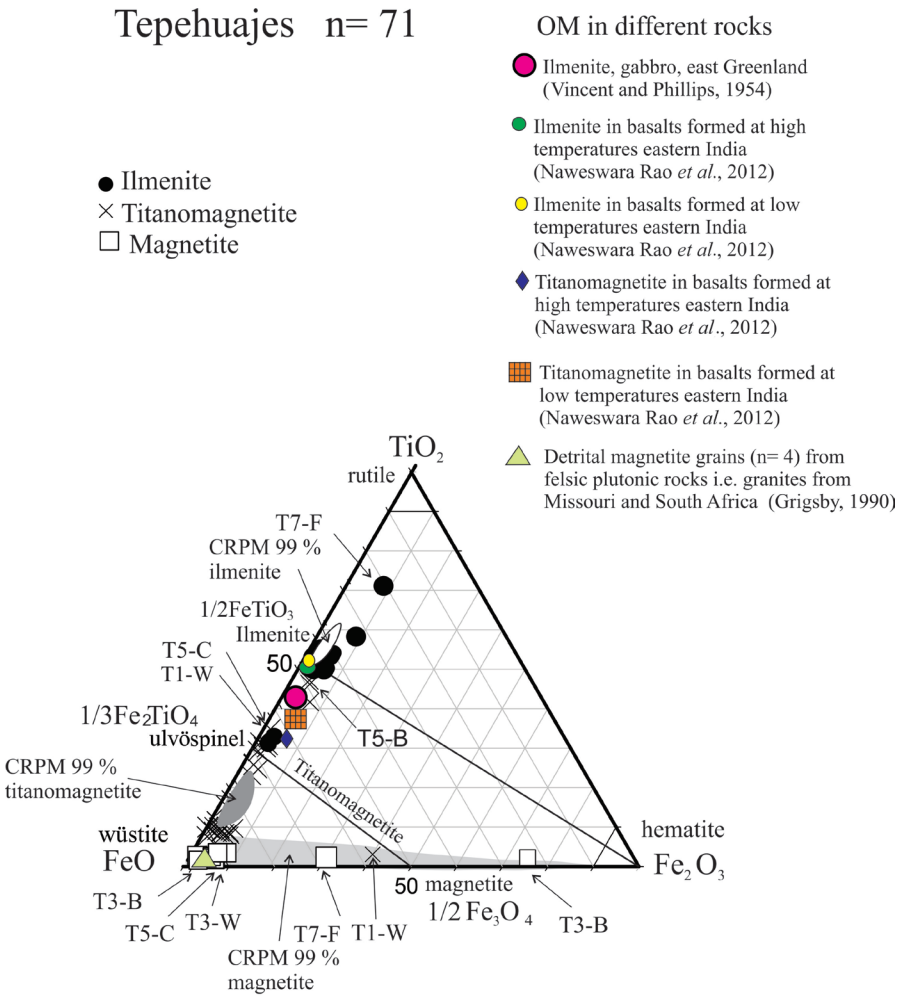

Figure 4. TiO_2-FeO-Fe_2O_3 ternary diagram for Tepehuajes beach and dune sands with ilmenite and titanomagnetite. Counted-grains n = 71. Ellipses are CRPM at 99 % confidence levels (Weltje, 2002). See text for explanation.

5. Discussion

5.1. Grain size

The average grain-size parameters for the three beach sites do not differ significantly. Grain size values similar to those of this study have been reported for the western coast of the Gulf of Mexico close to the area of influence of the Trans-Mexican Volcanic Belt (TMVB) where a wide coastal plain is exposed (Kasper-Zubillaga *et al*., 1999). In contrast, coarse grain-sized beach sands from the southwestern Mexican Pacific coast are influenced by volcanic outcrops in a narrow coastal plain (Carranza-Edwards *et al*., 2009). In our study, the grain sizes were determined by a wide coastal plain that controlled their distribution in beach and dune sands.

5.2. Modal analysis

The quartzose character of the beach and dune sands from the western coast of the Gulf of Mexico is a response to the control exerted by the sedimentary units, *i.e.*, Upper Cretaceous and Tertiary shales and sandstones, exposed along the coast from the Miramar to the Tepehuajes beach sites. This interpretation is supported by the presence of sedimentary rock fragments like sandstones, chert, monocrystalline quartz with straight extinction, K-feldspars, amphiboles, and pyroxenes as non-OM fractions from the whole bulk sand composition (Kasper-Zubillaga *et al*., 2013). Furthermore, it is likely that the gabbro and especially granite outcrops from the Sierra de Tamaulipas (Ortega-Gutiérrez *et al*., 1992; Aranda-Gómez *et al*., 2007) are the remnants of denudation processes that influenced

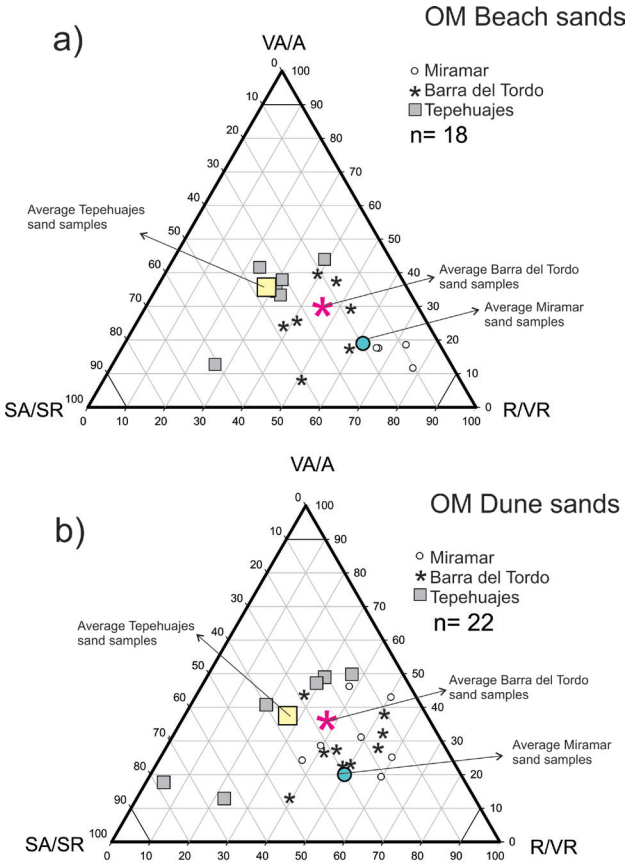

Figure 5. OM roundness ternary diagram with samples from Miramar, Barra del Tordo, and Tepehuajes a) beach sands; b) dune sands. Poles are VA/A, SA/SR, and R/VR. See text for major explanation.

the supply of sediments that contribute to the sedimentary units along the coast, *i.e*., the Upper Cretaceous and Tertiary shales and sandstones. Elsewhere, modern quartz-rich beach and dune sands are found derived from granite, *i.e.*, K-feldspar, albite Na-plagioclase enrichment, amphiboles, and mica, *e.g*., on the eastern coast of South America, the northwestern coast of Mexico and the northern coast of New Zealand, where sedimentary and acidic intrusive rock units control the major composition (Potter, 1986; Kasper-Zubillaga *et al*., 2005, 2007 a, b; Kasper-Zubillaga and Zolezzi-Ruiz, 2007).

5.3. OM content and roundness.

The OM content of the three beach sites increases from Miramar to Tepehuajes, from south to north. The increase in OM at the Tepehuajes beach sites may be due to the longshore transport of OM. This is supported by the fact that beach and dune sands are composed mainly of subrounded and rounded to very rounded ilmenite, titanomagnetite, and magnetite grains. This interpretation is based on the data for OM thin sections that were plotted in the VA/A-SA/SR-R/VR triangular diagram (Figures 5a, b). The roundness of the OM at each beach site is similar, tending towards the SA/SR and R/R/VR poles. This suggests a long time of transport along the coast due to longshore currents, breaking waves, and backflow concentration of OM landwards, as well as mixing with sea-floor sediments during river water-borne sand settlement seawards (Bradley, 2002; Mohapatra *et al*., 2015). Additionally, modern river-sand discharges exert little control on the current deposition of OM along the beaches studied (Kasper-Zubillaga *et al*., 2013).

5.4. OM at the Miramar beach site

Ilmenite is probably primarily derived from pre-existing eroded mafic sources, *i.e.*, alkali basalts close to the Miramar beach site (Cantagrel and Robin, 1979; Nageswara-Rao *et al*., 2012). This interpretation is closer to the basalt and alkali basalt outcrops near to the Miramar beach site. Evidence of these statements are based on a) the presence of alkali basalts as part of the outcrops of the remnants of the Aldama volcanic field, b) the increase of K-feldspar content as "light minerals" in the sands, c) the presence of quartz and pyroxenes in the Miramar sands, and d) the presence of light rare earth element (LREE) enrichment, *i.e.*, chondrite normalized and the positive Eu anomalies (Chakraborty *et al*., 1980; Nageswara-Rao *et al*., 2012; Kasper-Zubillaga *et al*., 2013). The ilmenite has not been subjected to chemical alteration, since its average TiO_2 and FeO values are below and above the average values obtained for altered ilmenite (intermediate phases) of 67.36 ± 7.50 and 27.31 ± 8.00, respectively, in sedimentary rocks (Morad and Aldahan, 1986). Additionally, relict, unaltered ilmenite detrital grains, *i.e.*, mostly subrounded, rounded, and very rounded homogeneous grains, from offshore marine sands may be transported onshore via longshore currents, breaking waves and wind deflation (Bradley *et al*., 2002) (Figures 5a, b).

Titanomagnetite is derived from sedimentary units such as the Upper Cretaceous and Tertiary shales and sandstones exposed as a result of the denudation of mafic/basalt rocks from the subalkaline to alkali basalts from the Aldama volcanic rocks (Vasconcelos *et al*., 2002) since the non-OM minerals included K-feldspars, amphiboles and pyroxenes and the chemical composition overlaps on the ulvöspinel mark. Titanomagnetite is a solid solution between the magnetite and the ulvöspinel end members (Sauerzapf *et al*., 2008). The main source of titanomagnetite is probably composed of alkali basalts and/or tholeiitic basalts, *i.e.*, subalkaline basalts (Vasconcelos *et al*., 2002) (Table 3). Furthermore, the Ti-Fe composition values (%) are close to values from tholeiitic basalts from eastern India and titanomagnetite homogeneous grains (Deer *et al*., 1966; Prévot and Mergoil, 1973; Nageswara-Rao *et al*., 2012) (Table 3). The presence of subordinate concentrations of sphene and zircon is derived as an exogenous process of granites forming part of the Sierra de Tamaulipas (Ortega-

Table 3. Average data ranges from the beach sites studied based on the TiO_2 and FeO percentages obtained by the MASP (see text for explanation). Comparisons were made for the low and high Ti-Fe percentages reported for basalt flows from eastern India (Nageswara-Rao *et al*., 2012).

	Miramar	Basalts*	Miramar	Basalts
Ilmenite	TiO2	TiO2	FeO	FeO
Average range (low to high)	51.41–54.27	50.62–51.95	42.9–45.90	48.43–49.38
Titanomagnetite				
Average range (low to high)	19.19–27.40	27.0–30.26	51.41–54.27	59.32–62. 43
Ilmenite	Barra del Tordo	Basalts	Barra del Tordo	Basalts
Average range (low to high)	49.19–56.05	50.62–51.95	39.46– 44.92	48.43–49.38
Titanomagnetite				
Average range (low to high)	17.82–31.67	27.0–30.26	17.82–31.67	59.32–62. 43
Ilmenite	Tepehuajes	Basalts	Tepehuajes	Basalts
Average range (low to high)	45.19–53.89	50.62–51.95	40.25–50.66	48.43–49.38
Titanomagnetite				
Average range (low to high)	8.41–26.15	27.0–30.28	66.32–85.76	59.32–62. 43

Average data in % from the semiquantitative MASP procedure. *Basalts = Tholeiitic basalts. Data taken from Nageswara-Rao *et al*. (2012).

Gutiérrez *et al*., 1992; Aranda-Gómez *et al*., 2007) as part of the composition of the sedimentary units described previously, *i.e*., Upper Cretaceous and Tertiary shales and sandstones.

5.5. OM at the Barra del Tordo beach site

Ilmenite grains at the Barra del Tordo site are also derived from sedimentary sources such as the Upper Cretaceous and Tertiary shales and sandstones as part of the outcrops of the remnants of the Aldama volcanic field. These grains are homogeneous, rounded to subrounded, with an average range of 40 to 48 % of FeO and 49 to 56 % of TiO_2, suggesting fresh ilmenite grains that come close to the composition of unaltered ilmenite minerals from sedimentary rocks (Morad and Aldahan, 1986). Beach processes such as breaking waves, longshore currents, and wind deflation control the transport and deposition of ilmenite grains onshore.

Titanomagnetite is also derived from the sedimentary units resulting from the erosion of subalkaline rocks (Vasconcelos *et al*., 2002). The primary sources of titanomagnetite are probably subalkaline basalts low in K-feldspar with increased Ca-plagioclase (Aranda-Gómez *et al*., 2007; Nageswara-Rao *et al*., 2012; Kasper-Zubillaga *et al*., 2013) (Tables 1 and 3). A subordinate low concentration of magnetite is observed in the Barra del Tordo beach and dune sands due to the absence of felsic volcanic mafic but dominantly acidic rocks as primary sources of the beach and dune sands, which can contribute to homogeneous magnetite grains (Grigsby, 1990).

5.6. OM at the Tepehuajes beach site

The OM concentration at the Tepehuajes beach site is the highest for beach and dune sands compared to the Miramar and Barra del Tordo beach locations. Major dispersion in the ilmenite plots is observed in the TiO_2-FeO-Fe_2O_3 ternary diagram, suggesting a large variation in the ilmenite grains probably due to the variable concentration of Fe-Ti oxides.

Ilmenite, titanomagnetite, and magnetite as subordinate components from the whole bulk composition of the beach and sand studied are derived from the Upper Cretaceous and Tertiary shales and sandstones units originated by the denudation of the Sierra de Tamaulipas, Aldama, and Sierra de Maratínez dominated by granites, trachytes, alkali basalts, and subalkaline basalts, *i.e.*, toleiitic basalts (Ortega-Gutiérrez *et al*., 1992; Vasconcelos *et al*., 2002; Aranda-Gómez *et al*., 2007) (Figures 6a, b).

A forward stepwise linear discriminant function analysis (LDFA) for the three beach sites showed that TiO_2 is the variable that contributes to the separation of some mineral samples from the three sites (significance $\rho = 0.00$; Wilks' lambda = 0.97; tolerance = 0.90) (Figure 7). The variable concentration of TiO_2 controls the dispersion in the composition of TiO_2 and FeO in the ilmenite, titanomagnetite, and magnetite grains for the three beaches studied based on the LDFA. The LDFA performed for the three sites shows how some of the Tepehuajes OM samples plot slightly away from the rest of the overlapped samples compared to the rest of the beach samples.

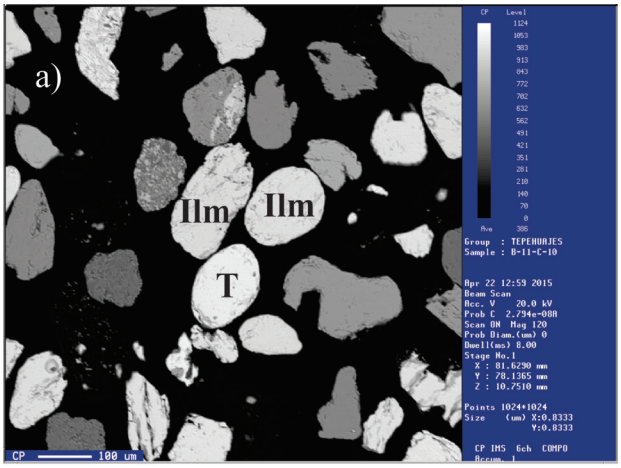

Figure 6a. Rounded to subrounded ilmenite and titanomagnetite grains. Sample B11-C, Barra del Tordo beach site. b) Magnetite with titanomagnetite lamellae. Sample T7-F, Tepehuajes beach site.

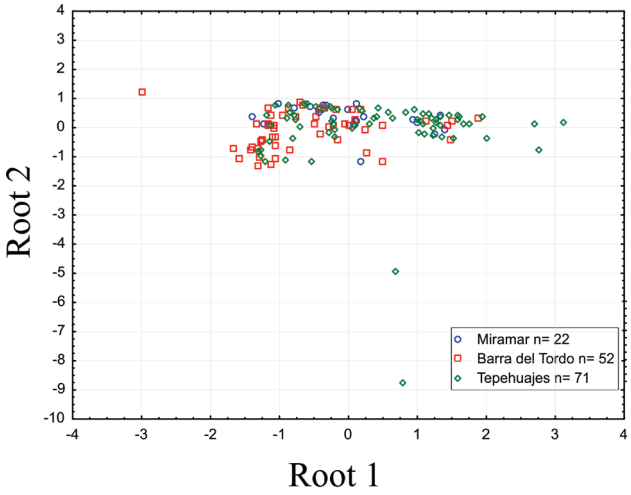

Figure 7. Forward stepwise linear discriminant function analysis (LDFA) for the three beach locations. Roots 1 and 2 represent the best linear fit when variables are reduced to roots.

6. Conclusion

Grain sizes in the sands from the western coast of the Gulf of Mexico are characterized by moderately to well-sorted fine sands controlled by a wide coastal plain. The beach and dune sands from the western coast of the Gulf of Mexico come from the Upper Cretaceous and Tertiary shales and sandstones exposed along the coast from the Miramar to the Tepehuajes beach sites. It is likely that eroded cycles from the Sierra de Tamaulipas composed of intrusive rocks produced the shale and sandstone units near the coast. Grain fractions such as sandstones, chert, monocrystalline quartz with straight extinction, K-feldspars, amphiboles and pyroxenes support the previous statement. The OM are composed of subordinate ilmenite, titanomagnetite, and magnetite derived from pre-existing eroded mafic sources, *i.e.*, alkali and subalkaline basalts from the Aldama and Sierra Maratínez volcanic field sites respectively and also from granites from the Sierra de Tamaulipas. Subrounded and rounded to very rounded OM grains like ilmenite, titanomagnetite, and magnetite, suggest longshore transport, breaking wave influence, and the wind deflation effect, from the source rock to the beach site.

Acknowledgements

This research was supported by the Instituto de Ciencias del Mar y Limnología, Universidad Nacional Autónoma de México, Internal Project (109). We thank Mr. Patrick Bennett Weill for English language review. We appreciate the reviews by Dr. Tobias Schwennicke and an anonymous reviewer for their comments and suggestions, which were so critical and essential to the improvement of the manuscript. This manuscript was part of PAPIIT Project No. INI112811-2. DGAPA. Universidad Nacional Autónoma de México.

References

Abuodha, J.O.Z., 2003, Grain size distribution and composition of modern dune and beach sediments, Malindi Bay coast, Kenya: Journal of African Earth Sciences, 36, 41–54.

Angusamy, N., 2006, Placer deposits of Southern Tamil Nadu Coast, India: Marine Georesources and Geotechnology, 24, 77–102.

Aranda-Gómez, J.J., Luhr, J.F., Housh, T., Valdez-Moreno, G., Chávez-Cabello, G., 2007, Late-Cenozoic intraplate-type volcanism in central and northern Mexico: a review, *in* Alaniz-Álvarez, S.A., Nieto-Samaniego, A.F., (eds.), Geology of Mexico: Celebrating the centenary of the Geological Society of Mexico, Boulder, Colorado, Geological Society of America Special Paper, 117–128.

Armstrong-Altrin, J.S., Lee, Y.I., Kasper-Zubillaga, J.J., Carranza-Edwards, A., Garcia, D., Nelson Ebye, G., Balaramf, V., Cruz-Ortiz, N.L., 2012, Geochemical composition of beach sands from the western Gulf of Mexico, Mexico: Implication for provenance: Chemie Der Erde. Geochemistry, 72, 345–362.

Blatt, H., 1967, Original characteristics of clastic quartz grains: Journal of Sedimentary Petrology, 37, 1031–1044.

Bradley, J.P., Chew, P.M., Wilkins, C.J., 2002, Transport and distribution of magnetite and ilmenite on Westland beaches of New Zealand; with comment on the accumulation of other high-density minerals: Journal of the Royal Society of New Zealand, 32, 169–181.

Butler, R.F., 1992, Paleomagnetism: Magnetic Domains to Geologic Terranes: Boston, Blackwell Scientific Publications, 319 p.

Cantagrel, J.M., Robin, C., 1979, K-Ar dating on Eastern Mexican volcanic rocks-relations between the andesitic and the alkaline provinces: Journal of Volcanology and Geothermal Research, 5, 99–114.

Carranza-Edwards, A., Kasper-Zubillaga, J.J., Rosales-Hoz, L, Morales de la Garza E., Lozano Santa-Cruz, R., 2009, Beach sand composition and provenance in a sector of the southwestern Mexican Pacific: Revista Mexicana de Ciencias Geológicas, 26, 433–447.

Chakraborty, K.R., Sita Ram, G., Barlian Aidid, S., 1980, Rare earth elements abundances in alkaline basaltic lavas of Kuantan, Peninsular Malaysia: Geological Society of Malaysia Bulletin, 13, 103–111.

Darby, D.A., Tsang, Y.W., 1987, Variation in ilmenite composition within and among drainage basins implications for provenance: Journal of Sedimentary Petrology, 57, 831–837.

Deer, W.A., Howie, R.A., Zussman, J., 1966, An Introduction to Rock Forming Minerals: New York, John Wiley, 696 p.

Dill, H.G., 2007, Grain morphology of heavy minerals from marine and continental placer deposits, with special reference to Fe–Ti oxides: Sedimentary Geology, 198, 1–27.

Fernández-Eguiarte, A, Gallegos-García, A., Zavala-Hidalgo, J., 1992, Oceanografía Física (Masas de Agua y Mareas de los Mares Mexicanos) IV.9.1, 1: 4000000, Atlas Nacional de México: México, Instituto de Geografía, Universidad Nacional Autónoma de México, 1 mapa.

Fletcher, W.K., Church, M., Walcott, J., 1992, Fluvial transport equivalence of heavy minerals in the sand size range: Canadian Journal of Earth Sciences, 29, 2017–2021.

Folk, L., 1980, Petrology of Sedimentary Rocks: Austin Texas, Hemphill, 182 p.

Franzinelli, E., Potter, P.E., 1982, Petrology, Chemistry, and texture of modern river sands, Amazon River System: The Journal of Geology, 91, 23–39.

Garzanti, E., 2016, From static to dynamic provenance analysis—Sedimentary petrology upgraded: Sedimentary Geology, 336, 3–13.

Grigsby, J.D., 1990, Detrital magnetite as a provenance indicator: Journal of Sedimentary Petrology, 60, 940–951.

He, J., Zhou, Y., 2014, Micro Characteristics of Chert in Volcanic rocks of Xiong'er Group in the Southern Part of the North China Craton: Acta Geologica Sinica, 88, 289–290.

Instituto Nacional de Estadística y Geografía (INEGI), 2012, Anuario de Estadísticas por Entidad Federativa, Technical Report, 681 p.

Kasper-Zubillaga, J.J., Carranza Edwards, A., Rosales-Hoz, L., 1999, Petrography and geochemistry of Holocene sands in the western Gulf of Mexico: implications for provenance and tectonic setting: Journal of Sedimentary Research, 69, 1002–1010.

Kasper-Zubillaga, J.J., Dickinson, W.W., Carranza Edwards, A., Hornelas-Orozco, Y., 2005, Petrography of quartz grains in beach and dune sands of Northland, North Island, New Zealand: New Zealand Journal of Geology and Geophysics, 48, 649–660.

Kasper-Zubillaga, J.J., Ortiz-Zamora, G.V., Dickinson, W.W., Urrutia-Fucugauchi, J., Soler-Arrechalde, A.M. 2007a, Textural and compositional controls on modern beach and dune sands, New Zealand: Earth Surface Processes and Landforms, 32, 366–389.

Kasper-Zubillaga, J.J., Zolezzi-Ruiz, H., 2007, Grain size, mineralogical and geochemical studies of coastal and inland dune sands from the El Vizcaino Desert, B.C. México: Revista Mexicana de Ciencias Geológicas, 24, 423–438.

Kasper-Zubillaga, J.J., Zolezzi-Ruiz, H., Carranza-Edwards, A., Girón García, P. Ortiz-Zamora, G.V., Palma, M., 2007 b , Sedimentological, modal analysis and geochemical studies of desert and coastal dunes, Altar Desert, NW México: Earth Surface Processes and Landforms, 32, 498–508.

Kasper-Zubillaga, J.J., Carranza-Edwards, A., Morton-Bermea, O., 2008 a, Heavy minerals and rare earth elements in coastal and inland dune ands of El Vizcaino Desert, Baja California Peninsula, Mexico: Marine Georesources & Geotechnology, 26, 172–188.

Kasper-Zubillaga, J.J., Acevedo-Vargas, B., Morton Bermea, O., Ortiz-Zamora, G., 2008 b, Rare earth elements of the Altar Desert dune and coastal sands, Northwestern Mexico: Chemie Der Erde Geochemistry, 68, 45–59.

Kasper-Zubillaga, J.J., 2009, Roundness in quartz grains from inland and coastal dune sands, Altar Desert, Sonora, Mexico: Boletín de la Sociedad Geológica Mexicana, 61, 1–14.

Kasper-Zubillaga, J.J., Armstrong-Altrin, J.S., Carranza-Edwards, A., Morton-Bermea, O., Lozano Santa Cruz, R., 2013, Control in beach and dune sands of the Gulf of Mexico and the role of nearby rivers: International Journal of Geosciences, 4, 1157–1174.

Kasper-Zubillaga, J.J., Arellano-Torres, E., Armstrong-Altrin, J.S., Sial A.N., 2015, A study of carbonate beach sands from the Yucatan Peninsula, Mexico: a case study: Carbonates and Evaporites. Published online, DOI 10.1007/s13146-015-0283-0.

Komar, P.D., Inman D.L., 1970, Longshore sand transport on beaches: Journal of Geophysical Research, 75, 5914–5827.

Komar, P.D., Wang, C., 1984, Processes of selective grain transport and the formation of placers on beaches: Journal of Geology, 92, 637–655.

Le Maitre, R.W., Streckeisen, A., Zanettin, B., Le Bas, M. J., Bonin, B., Bateman, P., Bellieni, G., Dudek, A., Efremova, S., Keller, J., Lameyre, J., Sabine, P.A., Schmid, R., Sorensen, H., Woolley, A.R., 2002, Igneous Rocks: A Classification and Glossary of Terms: Recommendations of the International Union of Geological Sciences Subcommission on the Systematics of Igneous Rocks: Cambridge, Cambridge University Press, 236 p.

Livingstone, I., Bullard, J.E., Wiggs, G.F.S., Thomas, D.S.G., 1999, Grain-size variation on dunes in the Southwest Kalahari, Southern Africa: Journal of Sedimentary Research, 69, 546–552.

Makvandi, S., Georges Beaudoin, G., McClenaghan, B.M., Layton-Matthews, D., 2015, The surface texture and morphology of magnetite from the Izok Lake volcanogenic massive sulfide deposit and local glacial sediments, Nunavut, Canada: Application to mineral exploration: Journal of Geochemical Exploration, 150, 84–103.

Mohapatra, S., Behera, P., Das, S.K., 2015, Heavy Mineral Potentiality and Alteration Studies for Ilmenite in Astaranga Beach Sands, District Puri, Odisha, India: Journal of Geoscience and Environment Protection, 3, 31–37.

Morad, S., Aldahan, A.A., 1986, Alteration of detrital Fe-Ti oxides in sedimentary rocks: Geological Society of America Bulletin, 97, 567–578.

Nageswara-Rao, P.V., Swaroop, P.C., Karimulla, S., 2012, Mineral chemistry of Pangidi basalt flows from Andhra Pradesh: Journal of Earth System Science, 121, 525–536.

Nallusamy, B., Babu, S., Suresh-Babu, D.S., 2013, Heavy Mineral Distribution and Characterisation of Ilmenite of Kayamkulam—Thothapally Barrier Island, Southwest Coast of India: Journal of Geological Society of India, 81, 129–140.

Ortega-Gutiérrez, F., Mitre-Salazar, L.M., Roldán-Quintana, J., Aranda-Gómez, J., Morán-Zenteno, D., Alaniz-Álvarez, S., Nieto-Samaniego, A., 1992, Carta Geológica de la República Mexicana 1:2000000: México, Universidad Nacional Autónoma de México, Instituto de Geología, Secretaría de Energía, Minas e Industria Paraestatal, Consejo de Recursos Minerales, 1 mapa.

Pérez-Villegas, G., 1990, Vientos Dominantes IV.4.2, escala 1:4000000: Atlas Nacional de México. Instituto de Geografía, Universidad Nacional Autónoma de México, Mexico, 1 mapa.

Potter, P.E., 1986, South America and a few grains of sand: part 1: beach sands: The Journal of Geology, 94, 301–319.

Powers, M.C., 1953, A new roundness scale for sedimentary particles: Journal of Sedimentary Petrology, 23, 117–119.

Prévot, M., Mergoil, J., 1973, Crystallization trend of titanomagnetites in an alkali basalt from Saint-Clément (Massif Central, France): Mineralogical Magazine, 39, 474–481.

Sagga, A.M.S., 1993, Roundness of sand grains of longitudinal dunes in Saudi Arabia: Sedimentary Geology, 87, 63–68.

Sauerzapf, U., Lattard, D., Burchard, M., Engelmann, R., 2008, The titanomagnetite-ilmenite equilibrium: new experimental data and thermooxybarometric application to the crystallization of basic to intermediate rocks: Journal of Petrology, 49, 1161–1185.

Treviño-Cázares, A., Ramírez-Fernández, J.A., Velasco-Tapia, F., Rodríguez-Saavedra, P., 2005, Mantle xenoliths and their host magmas in the Eastern Alkaline Province, Northeast Mexico: International Geology Review, 47, 1260–1286.

Vasconcelos, M., Ramírez-Fernández, J.A., Viera-Décida, F., 2002, Petrología del vulcanismo traquítico del complejo volcánico de Villa Aldama, Tamaulipas: Geos, 22, 250–251.

Vincent, E.A., Phillips, R., 1954, Iron-titanium oxide minerals in layered gabbros of the Skaergaard intrusion, East Greenland. Part I. Chemistry and ore-microscopy: Geochimica et Cosmochimica Acta, 6, 1–26.

Voll, G., 1960. New work on petrofabrics: Liverpool and Manchester: Geological Journal, 2, 503–567.

Weltje, G.J., 2002, Quantitative analysis of detrital modes: statistically rigorous confidence regions in ternary diagrams and their use in sedimentary petrology: Earth Science Review, 57, 211–253.

Yáñez-Arancibia, A., Day, J.W., 2005, Environmental sub-regions in the Gulf of Mexico Coastal Zone the ecosystem approach as an integrated management tool: Ocean and Coastal Management, 47, 727–757.

Manuscript received: August 19, 2015.
Corrected manuscript received: January 1, 2016.
Manuscript accepted: January 20, 2016.